



Role of proximal and distal tear size ratio in hemodynamic change of acute type A aortic dissection

Xiaonan Li¹, Huanyu Qiao¹, Yue Shi², Jinrong Xue¹, Tao Bai¹, Yongmin Liu¹, Lizhong Sun¹

¹Department of Cardiovascular Surgery, Beijing Anzhen Hospital of Capital Medical University, Beijing Institute of Heart, Lung and Blood Vessel Diseases, Beijing, China; ²School of Life Science and BioEngineering, Beijing University of Technology, Beijing, China

Contributions: (I) Conception and design: X Li, Y Liu, L Sun; (II) Administrative support: Y Liu, L Sun; (III) Provision of study materials or patients: J Xue, T Bai; (IV) Collection and assembly of data: X Li, H Qiao, Y Shi; (V) Data analysis and interpretation: X Li; (VI) Manuscript writing: All authors; (VII) Final approval of manuscript: All authors.

Correspondence to: Yongmin Liu. Department of Cardiovascular Surgery, Beijing Anzhen Hospital, Capital Medical University, No. 2 Anzhen Road, Beijing, China. Email: liuyongmin100@sina.com; Lizhong Sun. Department of Cardiovascular Surgery, Beijing Anzhen Hospital, Capital Medical University, No. 2 Anzhen Road, Beijing, China. Email: sunlizhong1960@sina.cn.

Background: Acute type A aortic dissection (ATAAD) is a life-threatening disease. The aim of this study was to examine the role of tear size in the hemodynamic change and help improve the treatment level of this extremely dangerous disease.

Methods: A total of 120 ATAAD patients treated in our institution from November 2014 to December 2016 were divided into three groups according to proximal and distal tear size ratio (PDTSR). There were 35 patients in group A (PDTSR $\geq 2:1$), 44 patients in group B ($1:2 < PDTSR < 2:1$), and 41 patients in Group C (PDTSR $\leq 1:2$). Three computational fluid dynamics (CFD) models with different PDTSRs were established to investigate the hemodynamic difference in the three groups.

Results: The mean age (\pm SD) of the 120 patients included in this study was 47.7 ± 10.1 years. Patients in Group A had a significantly larger proximal tear size (219.1 ± 76.5 vs. 127.7 ± 70.1 vs. 75.7 ± 49.7 mm²; $P < 0.001$). The mortality of the patients in group A was significantly higher than those in group B and group C in the acute phase (37.1% vs. 2.3% vs. 2.4%, respectively; $P < 0.001$). A proximal tear larger than a distal tear was found to be significantly associated with preoperative death in logistic regression analysis (odds ratio: 15.89; 95% confidence interval, 2.702–93.477; $P = 0.002$).

Conclusions: A proximal tear larger than a distal tear was associated with a significantly high-pressure difference between false and true lumens and more blood flow into the false lumen. In such cases, patients would experience extremely high mortality and morbidity.

Keywords: Acute type A aortic dissection (ATAAD); proximal tear size; distal tear size; computational fluid dynamics (CFD)

Submitted Apr 20, 2020. Accepted for publication Jun 04, 2020.

doi: 10.21037/jtd-20-1920

View this article at: <http://dx.doi.org/10.21037/jtd-20-1920>

Introduction

Acute type A aortic dissection (ATAAD) is a life-threatening condition for which early diagnosis, treatment, and close follow-up are critical for survival. The mortality rate of untreated ATAAD reaches 50% in the first 48 hours, and immediate surgical intervention is indicated after the

diagnosis (1-4). Within the last decades, techniques for complete aortic root replacement were applied and more recently aortic valve sparing root surgery (for example David and Yacoub technique) was introduced in ATAAD repair. Furthermore, synthetic vascular grafts with side branches and hybrid prosthesis have been evolved as reliable solutions for the dissected aortic arch and descending aorta.

However, the clinical manifestations and complications of ATAAD are protean, with multisystem involvement and a range of severity; therefore, not all patients can receive surgery in time.

As far as we know, hemodynamic forces play an important role in the pathogenesis of aortic dissection. Several studies have pointed out that ATAAD patients experience an extremely high operative mortality once hemodynamic instability emerges which is similar to what occurs with medical management alone (5-7). Although most hemodynamic parameters cannot be measured directly, the recent development of computer technology has enabled computational fluid dynamics (CFD) to be widely applied in the study of hemodynamics and has provided a novel way to elucidate the mechanism of aortic dissection. Several studies have reported that blood flow into the false lumen and false lumen pressure increase with the greater size of the primary tear (8,9). Although these numerical models could help us understand the relationships between the risks and tear size, the issue still needs clinical data validation to solve the practical clinical problems.

To our knowledge, no studies have investigated the role of tear size by correlating the CFD findings with clinical data of ATAAD. We believe both the proximal and distal tear size should be taken into consideration in evaluating the perioperative outcomes and hemodynamic changes. The purpose of our research was to summarize the clinical data of ATAAD patients with CFD simulation to verify the effectiveness of CFD and help explain the various clinical manifestations of ATAAD patients to improve the treatment level. We present the following article in accordance with the STROBE reporting checklist (available at <http://dx.doi.org/10.21037/jtd-20-1920>).

Methods

Patients

The study was conducted in accordance with the Declaration of Helsinki and was approved by the Beijing Anzhen Hospital of Capital Medical University (KS2019034) and written informed consent was obtained from all patients.

Patients with the radiologic diagnosis of ATAAD from November 2014 to December 2016 in our institution were identified. The diagnosis of ATAAD was established with computed tomography angiography (CTA) examinations after the onset of symptoms. According to the Stanford

University classification, type A aortic dissection was defined as an involvement of the ascending thoracic aorta and/or the aortic arch. Aortic dissection was defined as acute if chest pain and/or related symptoms were present within 14 days of the operation (1). CTA was performed with 64-slice scanners with intravenous injection of 80 to 120 mL of nonionic iodinated contrast material. Furthermore, the image was required to be clear enough for the measurement of aortic parameters, such as tear sizes and diameters of dissection, and those that were not were excluded. Patients only affected by the ascending aorta were excluded. Preoperative clinical variables were recorded, including patient demographics and history, clinical presentation, complications and mortality, and imaging results.

All procedures were carried out by a median sternotomy and total cardiopulmonary bypass (CPB) with selective cerebral perfusion (SCP). Cannulation of the right axillary artery was used for CPB and SCP. The arterial line was bifurcated for the right axillary artery and for antegrade perfusion through 1 limb of a 4-branch prosthetic graft. Aortic root procedures were done (if indicated) during cooling. Circulatory arrest was instituted if the nasopharyngeal temperature reached 18 to 22 °C. Unilateral SCP was started through the right axillary artery after the brachiocephalic arteries were cross-clamped and the brain was perfused.

Image analysis

To decrease the selection bias, CT images were evaluated by two experienced cardiac surgeons with >10 years of experience (Dr. Liu and Dr. Sun). Intimal tears were detected and measured at axial and sagittal views with CTA which scanned the entire aorta and the product of two diameters stands for the tear size (shown in *Figure 1*). Patients who had multiple proximal or distal tears were represented by the sum of the sizes. Patients were divided into three different groups according to the proximal and distal tear size ratio (PDTSR). Patients whose PDTSR was $\geq 2:1$ were defined as group A, patients whose PDTSR was between 1:2 and 2:1 were defined as group B, and patients whose PDTSR was $\leq 1:2$ were defined as group C.

Numerical model creation

The numerical model of the aorta dissection was established based on the CTA data of a normal aorta. A semi-automatic threshold-based segmentation tool (Mimics17.0, Materialise

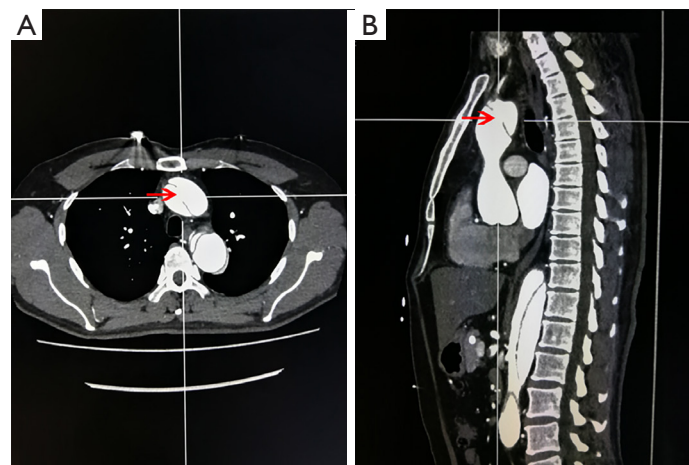


Figure 1 Measurement of tear (arrow) size. (A) Diameter at axial view; (B) diameter at sagittal view.

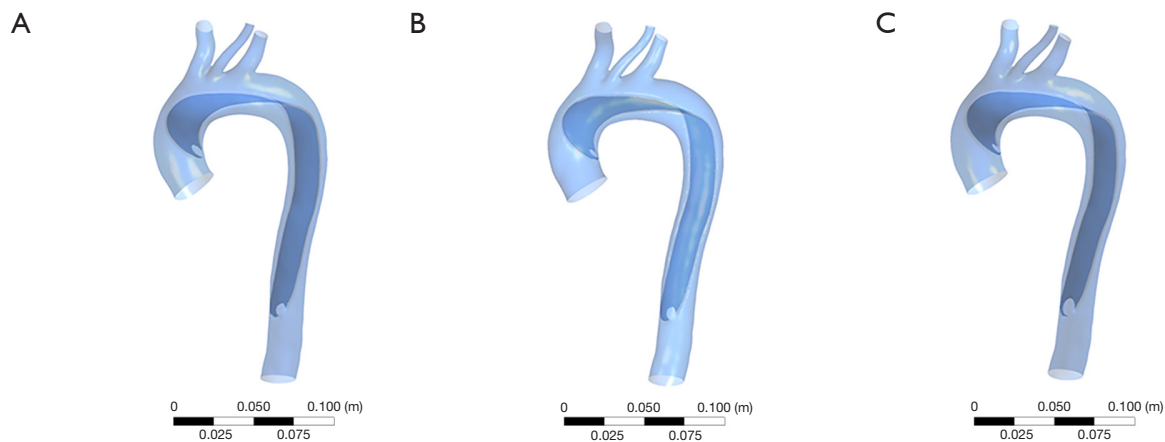


Figure 2 Three Stanford type A aortic dissection digital models of different proximal and distal tear sizes: model A, model B, and model C stand for group A, group B, and group C, respectively.

Inc., Belgium) was used to complete the image segmentation and surface reconstruction of the normal aorta. The models were exported into the stereolithographic (STL) file format after smoothing. The format of aorta models was changed into X_T by using the exact surface function (Geomagic Wrap 2015, Geomagic Inc., USA). Starting from the middle of the ascending aorta to the end of the thoracic aorta, a thin 1.2-mm thick layer was cut from the aorta model along the aorta axis to be used as the dissection flap. The modification of tear size and location was performed using an extruded boss feature and a computer-aided design (CAD) tool (SolidWorks 2015, SolidWorks Inc., France). The final models are shown in *Figure 2*. The proximal and distal tear sizes of three models were set according to the

CT measurement results which are shown in *Table 1*.

Mesbing and elements

A semi-automatic adaptive meshing technique was employed in HyperMeshv10.0 (Altair HyperWorks, Troy, MI, USA) to optimize both computational efficiency and element quality. Four-noded tetrahedral elements were assigned to all models, and the element size was set to 0.001 m. The grid was divided into various entrances, exits, and intimal regions.

Boundary conditions and flow models

The Navier-Stokes equations were solved numerically

Table 1 Preoperative patient data

Variable	Total (n=120)	Group A (n=35)	Group B (n=44)	Group C (n=41)	P value
Age, years	47.7±10.1	49.9±7.3	45.6±10.7	48.1±11.1	0.169
Male	83 (69.2)	22 (62.9)	34 (77.3)	27 (65.9)	0.326
Hypertension	93 (77.5)	28 (80)	33 (75.0)	32 (78.1)	0.891
Diabetes mellitus	5 (4.2)	2 (5.7)	1 (2.3)	2 (4.9)	0.736
CAD	5 (4.2)	1 (2.9)	1 (2.3)	3 (7.3)	0.524
Smoking history	43 (35.8)	15 (42.9)	14 (31.8)	14 (34.1)	0.621
Marfan syndrome	8 (6.7)	2 (5.7)	3 (6.8)	3 (7.3)	1.000
Proximal tear size, mm ²	130.8±85.2	219.1±76.5	127.7±70.1	75.7±49.7	<0.001
Distal tear size, mm ²	110.5±63.3	71.9±43.2	114.1±60.6	131.3±70.1	<0.001
Preoperative death	15 (12.5)	13 (37.1)	1 (2.3)	1 (2.4)	<0.001
Coma/stroke	7 (5.8)	4 (11.4)	2 (4.5)	1 (2.4)	0.289
Paraplegia	2 (1.7)	2 (5.7)	0 (0)	0 (0)	0.150
Tamponade	5 (4.2)	3 (8.6)	1 (2.3)	1 (2.4)	0.381
Mesenteric ischemia	4 (3.3)	2 (5.7)	1 (2.3)	1 (2.4)	0.681
Limb ischemia	14 (11.7)	5 (14.3)	5 (11.4)	4 (9.8)	0.880

Values are mean ± SD or number (%). CAD, coronary artery disease.

with a commercial finite-volume-based CFD solver (Fluent 15.0, Ansys, Inc., USA). Transient analysis was adopted to investigate the pulsatility of blood flow. Inlet flow waveforms for the ascending aorta were based on data presented by Mills *et al.* (10). The time-dependent pulsatile waveforms of flow at the descending aorta outlet, the brachiocephalic artery outlet, the left subclavian artery outlet, and the left common carotid artery outlet were obtained from the work of Olufsen *et al.* (11). We considered the blood to be incompressible and to have the same kinematic viscosity and density of Newtonian fluid with a dynamic viscosity of 3.5 m Pa and a density of 1,050 kg/m³. The aortic wall was assumed to be rigid, and therefore a no-slip condition was applied to the aortic wall. The calculation time-step and cardiac cycle were set to 0.01 and 0.8 seconds, respectively. The maximum root mean square residual was set as 10⁻⁵, and the maximum number of iterations per time step was set to 200 to ensure sufficiently accurate results. To minimize the influence of initial flow conditions, all simulations were carried out for 4 cardiac cycles to achieve a periodic solution, and the results presented here were obtained in the fourth cycle.

Statistical analysis

Continuous variables are reported as mean and standard deviation, and categorical data are reported as count and percentage. The *t*-test was selected to compare the differences between two groups in continuous variables. Pearson's χ^2 test and Fisher's exact test were selected to compare the differences in categorical variables between the three groups. We conducted binary logistic regression analysis to investigate the risk factors for the pre-operative death of ATAAD patients; P values <0.1 in univariate Analysis were input into multivariate analysis. In all tests, a P value <0.05 was considered significant. All calculations were performed using SPSS 25.0 (IBM Corporation, Chicago, USA).

Results

Clinical data

During the period from November 2014 to December 2016, 120 patients who were diagnosed with ATAAD based on an initial CTA scan performed at our institution were selected. Many other patients were transferred to our institution on the

Table 2 Operative data and postoperative outcomes

Variable	Total (n=105)	Group A (n=22)	Group B (n=43)	Group C (n=40)	P value
Bentall procedure	47 (44.8)	14 (63.6)	18 (41.9)	15 (37.5)	0.130
Ascending aorta replacement	58 (55.2)	8 (36.4)	25 (58.1)	25 (62.5)	0.130
CABG	11 (10.5)	3 (7.0)	2 (9.1)	6 (15.0)	0.503
Reconstruction of the sinus of valsalva	4 (3.8)	2 (9.1)	0 (0)	2 (5.0)	0.679
CPB time	220.9±54.3	225.7±54.2	211.7±46.5	220.7±58.3	0.621
SCP time	24.1±9.3	24.9±8.9	24.0±11.5	23.1±8.5	0.665
Cross-clamping time	124.7±34.5	123.1±30.1	126.1±43.4	125.8±34.4	0.919
30-day mortality	12 (11.4)	3 (13.6)	2 (4.7)	7 (17.5)	0.091
Stroke	9 (8.6)	3 (13.6)	0 (0)	6 (15.0)	0.014
Paraplegia	8 (7.6)	3 (13.6)	1 (2.3)	4 (10.0)	0.171
Acute renal failure	21 (20.0)	7 (31.8)	4 (9.3)	10 (25.0)	0.061
Ventilator support >5 days	26 (24.8)	11 (50.0)	8 (18.6)	7 (17.5)	0.006
Return to operating room for bleeding	10 (9.5)	2 (9.1)	5 (11.6)	3 (7.5)	0.910

Values are mean ± SD or number (%). CABG, coronary artery bypass graft surgery; CPB, cardiopulmonary bypass; SCP, selective cerebral perfusion.

basis of CTA images; as these initial scans were not readily available for measurement of the tear sizes, these patients were not included in this study. According to the ratio of proximal and distal tear size, 35 patients were included in group A, 44 patients in group B, and 41 patients in group C.

The preoperative clinical characteristics of ATAAD patients are summarized in *Table 1*. The mean age (± SD) of the 120 patients in this study was quite young (47.7±10.1 years). The majority of patients (69.1%) were male, and most patients (77.5%) had a history of hypertension. In our study, 8 patients had Marfan syndrome which is a multisystem connective tissue disorder with primary involvement of the cardiovascular, ocular, and skeletal systems. In group A, the patients had a significantly larger proximal tear (219.1±76.5 vs. 127.7±70.1 vs. 75.7±49.7 mm²; P<0.001). While the distal tear sizes were smaller in group A (71.9±43.2 vs. 114.1±60.6 vs. 131.3±70.4 mm²; P=0.001), other variables were generally similar between the three groups.

Of the 120 patients, 15 patients died before the surgery, while the other 105 patients received emergency surgeries. The pre-operative mortality of patients in group A was significantly higher than that in group B and group C in the acute phase (37.1% vs. 2.3% vs. 2.4%, respectively; P<0.001). At the same time, the complication rate was

higher in Group A, though this difference was not significant according to Pearson's χ^2 test (37.1% vs. 18.1% vs. 26.8%, respectively; P=0.171). Pre-operative mortality and complications are shown in *Table 1*.

All 105 patients underwent total arch replacement, 47 patients underwent the Bentall procedure, and 58 patients underwent ascending aorta replacement. Furthermore, 12 patients died within 30 days after the surgery (3 vs. 4 vs. 5, respectively; P=0.319). The rate of ventilator support lasting >5 days was significantly higher in group A (50% vs. 18.6% vs. 17.5%; P=0.006). Closure rate of the false lumen 3 months after the surgery was also higher in Group A, but the difference was not significant (85% vs. 65% vs. 72.7%, respectively; P=0.263). Perioperative data are shown in *Table 2*.

We also analyzed the predictors of preoperative death of ATAAD patients (*Table 3*). Proximal tear size larger than the distal tear was significantly associated with preoperative death of the ATAAD patients in multivariate analysis [odds ratio (OR): 15.89; 95% confidence interval (CI), 2.702–93.477; P=0.002].

Numerical simulation

Flow patterns

Velocity at peak systole data are presented in *Figure 3A*.

Table 3 Predictors of preoperative death

Variable	Univariate analysis			Multivariate analysis		
	OR	95% CI	P value	OR	95% CI	P value
Age	1.033	0.975–1.095	0.271			
Gender	2.995	0.996–9.006	0.051	1.769	0.394–7.941	0.456
Hypertension	0.530	0.164–1.711	0.288			
CAD	1.804	0.188–17.309	0.609			
Diabetes mellitus	5.231	0.798–34.280	0.085	5.274	0.410–67.842	0.202
Smoking history	1.225	0.405–3.710	0.719			
Alcohol	0.580	0.122–2.765	0.495			
WBC	1.079	0.997–0.168	0.058	1.073	0.960–1.200	0.214
Hemoglobin	0.767	0.566–1.039	0.086	0.735	0.488–1.108	0.142
Creatinine	1.004	0.993–1.005	0.462			
Tnl	1.041	0.877–1.236	0.648			
Proximal tear size	1.004	1.002–1.007	0.001	1.002	0.999–1.005	0.133
Distal tear size	0.992	0.983–1.002	0.122			
Proximal tear size larger than distal size	24.523	5.147–116.831	<0.001	15.893	2.702–93.477	0.002

CAD, coronary artery disease; WBC, white blood cell; OR, odds ratio; CI, confidence interval.

In the true lumen, turbulence of flow appeared near the aortic arch in all models. The same situation was observed in the false lumen, and the vortex phenomenon became more significant when the blood flow rate became lower. This phenomenon was similar to blood flow patterns observed in previous studies (12). In the whole pulse period, the blood flow velocity of the true lumen was faster than that in the false lumen. When the blood flowed from the aortic arch to the descending thoracic aorta, the peak value of the velocity gradually deviated from the medial wall, and the velocity was found to accelerate when passing through proximal and distal tears.

The flow rate of the false lumens was significantly different between the three models. With a large proximal tear and a small distal tear, blood flow in the false lumen was much greater in model A than that in model B and model C (42.98% vs. 29.23% vs. 26.63%). This would lead to a trend of continual expansion of the dissection and compression on the true lumen (13,14).

Time-averaged shear stress (TAWSS)

TAWSS is obtained by averaging the wall shear stress in a cardiac cycle. The distribution is shown in *Figure 3B*, and the three models do not differ from each other very much. TAWSS gradually decreases from the ascending aorta to the distal end

and partially elevates around the intimal tears. The wall TAWSS of the true and false lumen varies greatly throughout the cardiac cycle, and the TAWSS in the true lumen is higher than that in the false lumen and has a greater variation range.

Pressure distribution

The pressure distribution of the aortic wall at peak systole is shown in *Figure 3C*. The wall pressure gradually decreased from the ascending aorta to the distal end. Furthermore, the high wall pressure of ascending aorta and proximal descending aorta indicates that these sites may be dangerous areas of rupture. The false lumen wall pressure of both models was consistently higher than that of the true lumen. *Figure 4* shows the pressure difference of the two sides along the intima. When the pressure difference was significantly higher in model A, which had a larger proximal tear, the true lumen in model A would be compressed more seriously. This helps explain the higher mortality and morbidity in the group A patients. Continuous compression on the intimal wall may lead to structural damage and the stiffness and elasticity changes of the aortic wall, and eventually worsen the prognosis of patients. At the same time, the wall pressure difference changed considerably along the intima and showed a strong pulsation. The shrinking and

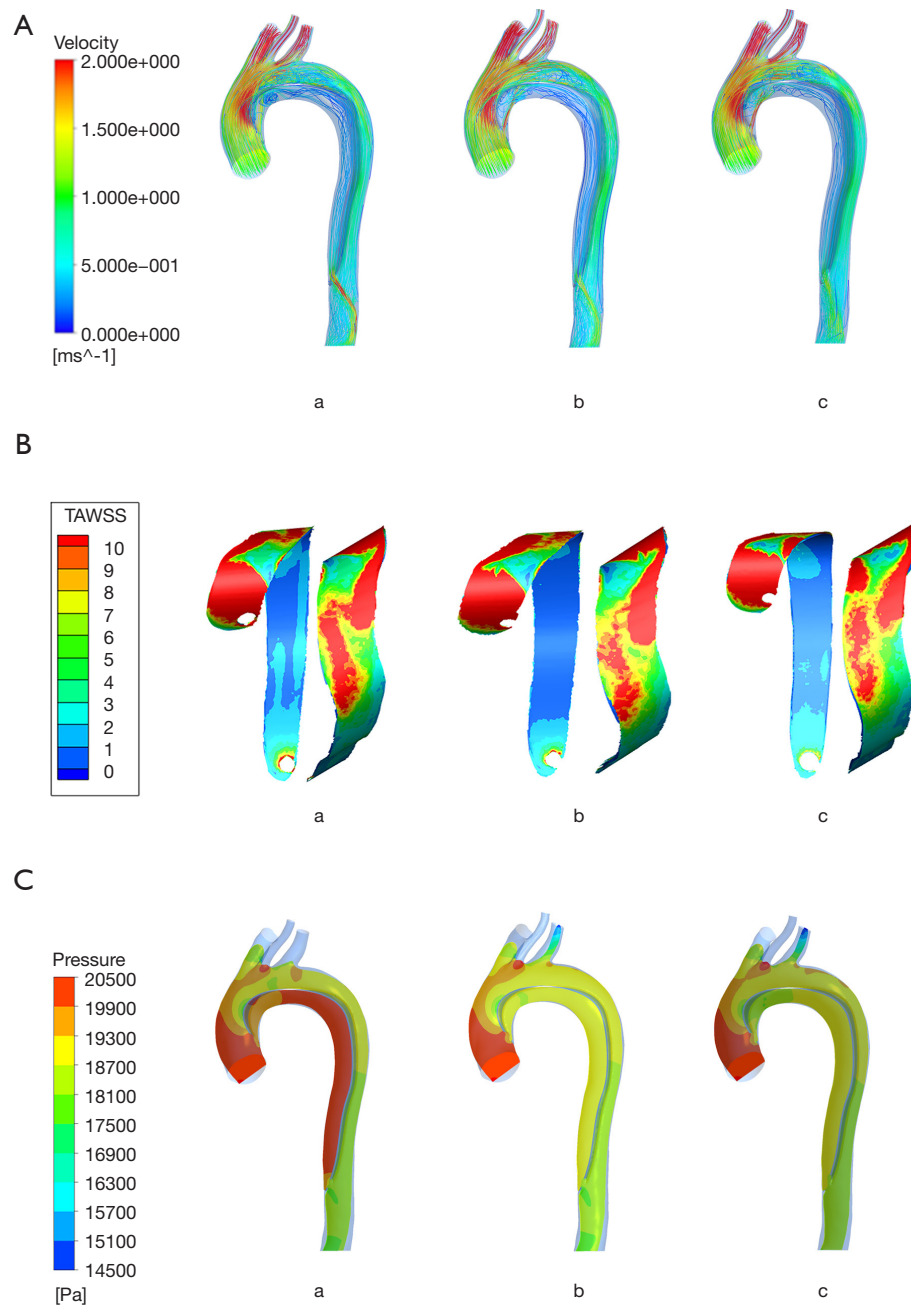


Figure 3 Flow velocity maps, wall pressure, and TAWSS on the intima at systolic peak: (A) flow velocity maps of the three models; (B) TAWSS contour plots of the intima of the three models; (C) pressure distributions at systolic peak. TAWSS, time-averaged shear stress.

stretching of the intima to adapt to the pressure changes would cause the emergence of re-entry tears.

Discussion

ATAAD results from a tear in the aortic intima, which

allows a pressurized hematoma to form within the media between the inner two-thirds and outer one-third of the aorta. The blood typically propagates rapidly along the length of the aorta and often compromises branch vessels along its path. The intimal tear plays a crucial role in the occurrence and progress of ATAAD, and the main purpose

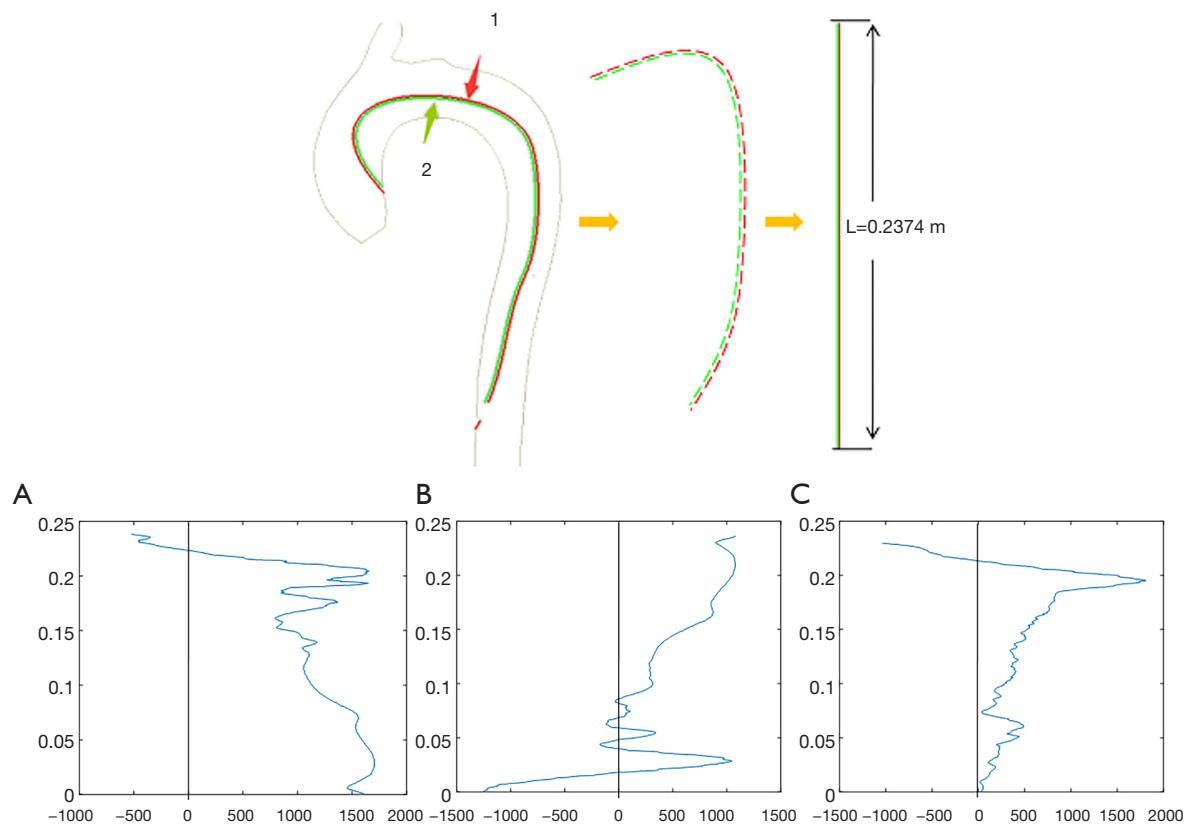


Figure 4 Pressure difference between the false and true lumen at systolic peak (Pa): Line 1: true lumen side of intima; Line 2: false lumen side of intima; (A) pressure difference in model A; (B) pressure difference in model B; (C) pressure difference in model C. Ordinate represents the intimal length, and abscissa represents the pressure difference (false lumen pressure–true lumen pressure).

of open surgery is to exclude the intimal tears (14-16). It was reported that type B aortic dissection patients with entry tear size ≥ 10 mm presented a higher incidence of dissection-related events and median growth rate than those with entry tear size 10 mm (17). Experimental studies have shown that a larger entry tear and inadequate outflow from the false lumen in type B aortic dissection would lead to a significant increase in mean arterial and diastolic pressure (9). However, all these studies focused on type B aortic dissection, which had better in-hospital survival than type A aortic dissection in the acute phase, and there was a paucity of studies investigating the hemodynamic changes in ATAAD patients. The incidence of type A aortic dissection was higher than type B aortic dissection, and patients with type A aortic dissection suffer double the mortality of individuals presenting with type B aortic dissection (25% and 12%, respectively) (1). Thus, our study aimed to investigate the role of PDTSR in hemodynamic changes of ATAAD patients by combining the CFD simulation with

clinical data.

According to Mehta *et al.*, abrupt onset of chest pain, hypotension, shock, and tamponade have been demonstrated to be predictors of in-hospital death in ATAAD patients (18). However, the morphologic cause of these complications still remains unknown. Our study collected the preoperative data of ATAAD patients with different PDTSR, and the results showed that patients whose proximal tear was larger than their distal tear would experience a significantly higher mortality and morbidity. The results of CFD gave us a better understanding of the clinical data and helped us to understand the hemodynamic changes of ATAAD patients. Patients with a larger proximal tear (model A) experienced a higher pressure difference between the false and true lumen and a higher percentage of total aortic flow diverted into the false lumen. In this case, the false lumen continued to expand, and the patients were more prone to persistent chest pain and severe complications. To decrease the compression on true lumen

and avoid aortic rupture, patients with a larger proximal tear may need stricter antihypertensive therapy during the perioperative period and more urgent surgical treatment. Moreover, we also noticed that the number of patients in group A was apparently smaller than that of group B and C. This indicates that patients with larger proximal tears were less likely to survive before arriving at the emergency room because of the early emergence of hemodynamic instability and sudden aortic rupture.

Wall shear stress has been implicated in initial aneurysm formation (19), but its role in aneurysmal pathogenesis and evolution is unclear. Aortic and intracranial aneurysm growth has been seen in both low wall shear stress conditions and high wall shear stress conditions (20-22). In the present study, high TAWSS was observed in both models from the ascending aorta to the proximal descending aorta, with the change of tear size having no impact. High TAWSS in the ascending aorta may be the reason why type A aortic dissection accounts for a significant proportion of aortic dissections (23,24).

Patients in group B and C were relatively more stable than those in group A during the preoperative period. We found out that it was the PDTSR, and not just the size of proximal or distal tear size, that decided the clinical outcomes of the patients. Consequently, patients whose proximal tear is larger than their distal one would benefit more from emergency surgery in order to avoid preoperative hemodynamic instability and aortic rupture. We also noticed that the 3-month closure rate of the false lumen was higher in group A (85% vs. 65% vs. 72.7%, respectively; $P=0.263$), though the difference was not significant. In the postoperative period, the large distal tears turned into entry tears, which would lead to more blood flow being diverted into the false lumen, and in this way the false lumen would stay patent in the follow-up time. We speculate that the remaining large distal tears of patients in group B would lead to a patent or partial false lumen during the post-operative follow-up period which has been demonstrated to be related to unfavorable prognosis after surgical repair (14,16,17,25,26). In this case, those patients with larger proximal tears (group A) may benefit from early intervention and develop the prognosis avoid re-operation, although this speculation requires further confirmation by further study.

Some limitations to this research should be addressed. First, the aortic wall was assumed to be rigid and the deformation of vessel was ignored. Second, as the source of dissection geometry was CTA imaging, both models

were subjected to identical inflow and outflow conditions. Although magnetic resonance angiography may provide more hemodynamic parameters, CTA remains the most common diagnostic imaging type performed in most type A aortic dissection patients. Third, the pixel widths of CT scans were not exactly the same, so some small tears might not have been detected. Finally, as not all CTAs were clear enough and most patients were transferred without initial CTA data making a measurement of the tear size impossible, our cohort size was relatively small.

Conclusions

A proximal tear significantly larger than a distal tear was associated with significantly different pressure difference between the false and true lumens and more blood flow into the false lumen. In this case, patients would experience extremely high mortality and morbidity and benefit from urgent surgery to fix the aortic dissection. These preliminary results demonstrated that computational aortic flow simulations can be used to clarify the pathogenesis of aortic dissection and help predict the clinical outcomes of ATAAD.

Acknowledgments

Funding: This work was funded by the Beijing Municipal Science & Technology Commission (Grant No. Z191100006619094).

Footnote

Reporting Checklist: The authors have completed the STROBE reporting checklist. Available at <http://dx.doi.org/10.21037/jtd-20-1920>

Data Sharing Statement: Available at <http://dx.doi.org/10.21037/jtd-20-1920>

Conflicts of Interest: All authors have completed the ICMJE uniform disclosure form (available at <http://dx.doi.org/10.21037/jtd-20-1920>). The authors have no conflicts of interest to declare.

Ethical Statement: The authors are accountable for all aspects of the work in ensuring that questions related to the accuracy or integrity of any part of the work are appropriately investigated and resolved. The study was

conducted in accordance with the Declaration of Helsinki and was approved by the Beijing Anzhen Hospital of Capital Medical University (KS2019034) and written informed consent was obtained from all patients.

Open Access Statement: This is an Open Access article distributed in accordance with the Creative Commons Attribution-NonCommercial-NoDerivs 4.0 International License (CC BY-NC-ND 4.0), which permits the non-commercial replication and distribution of the article with the strict proviso that no changes or edits are made and the original work is properly cited (including links to both the formal publication through the relevant DOI and the license). See: <https://creativecommons.org/licenses/by-nc-nd/4.0/>.

References

1. Erbel R, Aboyans V, Boileau C, et al. 2014 ESC Guidelines on the diagnosis and treatment of aortic diseases: Document covering acute and chronic aortic diseases of the thoracic and abdominal aorta of the adult. The Task Force for the Diagnosis and Treatment of Aortic Diseases of the European Society of Cardiology (ESC). *Eur Heart J* 2014;35:2873-926.
2. Di Tommaso L, Giordano R, Di Tommaso E, et al. Treatment with transfemoral bare-metal stent of residual aortic arch dissection after surgical repair of acute type an aortic dissection. *J Thorac Dis* 2018;10:6097-106.
3. Wu ZY, Li P, Wang JY, et al. Aortic intimal intussusception during acute type B aortic dissection endovascular repair. *Ann Transl Med* 2019;7:700.
4. Dib B, Seppelt PC, Arif R, et al. Extensive aortic surgery in acute aortic dissection type A on outcome - insights from 25 years single center experience. *J Cardiothorac Surg* 2019;14:187.
5. Conway BD, Stamou SC, Kouchoukos NT, et al. Effects of Hemodynamic Instability on Early Outcomes and Late Survival Following Repair of Acute Type A Aortic Dissection. *Aorta (Stamford)* 2014;2:22-7.
6. Trimarchi S, Nienaber CA, Rampoldi V, et al. Contemporary results of surgery in acute type A aortic dissection: The International Registry of Acute Aortic Dissection experience. *J Thorac Cardiovasc Surg* 2005;129:112-22.
7. Wei J, Chen Z, Zhang H, et al. In-hospital major adverse outcomes of acute Type A aortic dissection. *Eur J Cardiothorac Surg* 2019;55:345-50.
8. Cheng Z, Riga C, Chan J, et al. Initial findings and potential applicability of computational simulation of the aorta in acute type B dissection. *J Vasc Surg* 2013;57:35S-43S.
9. Rudenick PA, Bijmens BH, Garcia-Dorado D, et al. An in vitro phantom study on the influence of tear size and configuration on the hemodynamics of the lumina in chronic type B aortic dissections. *J Vasc Surg* 2013;57:464-74.e5.
10. Mills CJ, Gabe IT, Gault JH, et al. Pressure-flow relationships and vascular impedance in man. *Cardiovasc Res* 1970;4:405-17.
11. Olufsen MS, Peskin CS, Kim WY, et al. Numerical simulation and experimental validation of blood flow in arteries with structured-tree outflow conditions. *Ann Biomed Eng* 2000;28:1281-99.
12. Iliceto S, Nanda NC, Rizzon P, et al. Color Doppler evaluation of aortic dissection. *Circulation* 1987;75:748-55.
13. Tsai TT, Schlicht MS, Khanafer K, et al. Tear size and location impacts false lumen pressure in an ex vivo model of chronic type B aortic dissection. *J Vasc Surg* 2008;47:844-51.
14. Sharif M, Yap ZJ, Ghazal A, et al. Tear Size and Location Influence the Pressure of False Lumen Following Type A Aortic Dissection: Perspective of Current Evidence. *Heart Lung Circ* 2020;29:178-87.
15. Nishida H, Tabata M, Fukui T, et al. Surgical Strategy and Outcome for Aortic Root in Patients Undergoing Repair of Acute Type A Aortic Dissection. *Ann Thorac Surg* 2016;101:1464-9.
16. Bing F, Rodiere M, Martinelli T, et al. Type A acute aortic dissection: why does the false channel remain patent after surgery? *Vasc Endovascular Surg* 2014;48:239-45.
17. Evangelista A, Salas A, Ribera A, et al. Long-term outcome of aortic dissection with patent false lumen: predictive role of entry tear size and location. *Circulation* 2012;125:3133-41.
18. Mehta RH, Suzuki T, Hagan PG, et al. Predicting death in patients with acute type a aortic dissection. *Circulation* 2002;105:200-6.
19. Meng H, Wang Z, Hoi Y, et al. Complex hemodynamics at the apex of an arterial bifurcation induces vascular remodeling resembling cerebral aneurysm initiation. *Stroke* 2007;38:1924-31.
20. Bousset L, Rayz V, McCulloch C, et al. Aneurysm growth occurs at region of low wall shear stress: patient-specific correlation of hemodynamics and growth in a longitudinal study. *Stroke* 2008;39:2997-3002.
21. Sugiyama S, Meng H, Funamoto K, et al. Hemodynamic analysis of growing intracranial aneurysms arising from

- a posterior inferior cerebellar artery. *World Neurosurg* 2012;78:462-8.
22. Wu D, Shen YH, Russell L, et al. Molecular mechanisms of thoracic aortic dissection. *Journal of Surgical Research* 2013;184:907-24.
 23. Pape LA, Awais M, Woznicki EM, et al. Presentation, Diagnosis, and Outcomes of Acute Aortic Dissection: 17-Year Trends From the International Registry of Acute Aortic Dissection. *J Am Coll Cardiol* 2015;66:350-8.
 24. Carpenter SW, Kodolitsch YV, Debus ES, et al. Acute aortic syndromes: definition, prognosis and treatment options. *J Cardiovasc Surg (Torino)* 2014;55:133-44.
 25. Desai D, Miranda W, Connolly H, et al. Flow dynamics in the false lumen in distal aorta following surgery for type A aortic dissection. *Eur Heart J* 2019;40:561.
 26. Higashigaito K, Sailer AM, van Kuijk SMJ, et al. Aortic growth and development of partial false lumen thrombosis are associated with late adverse events in type B aortic dissection. *J Thorac Cardiovasc Surg* 2019. [Epub ahead of print].

Cite this article as: Li X, Qiao H, Shi Y, Xue J, Bai T, Liu Y, Sun L. Role of proximal and distal tear size ratio in hemodynamic change of acute type A aortic dissection. *J Thorac Dis* 2020;12(6):3200-3210. doi: 10.21037/jtd-20-1920